Low-Metallicity Star Formation:
From the First Stars to Dwarf Galaxies
Proceedings IAU Symposium No. 255, 2008
L.K. Hunt, S. Madden & R. Schneider, eds.

doi:10.1017/S1743921308024927

The Gas Phase in a Low Metallicity ISM

Elias Brinks[1], Se–Heon Oh[2], Ioannis Bagetakos[1], Frank Bigiel[3], Adam Leroy[3], Antonio Usero[1], Fabian Walter[3], W. J. G. de Blok[4], and Robert C. Kennicutt, Jr.[5]

[1]Centre for Astrophysics Research, University of Hertfordshire, Hatfield AL10 9AB, UK
[2]Research School of Astronomy & Astrophysics, The Australian National University, Mount Stromlo Observatory, Cotter Road, Weston Creek, ACT 2611, Australia
[3]Max–Plank–Institut für Astronomie, Königstuhl 17, 69117, Heidelberg, Germany
[4]Univ. of Cape Town, Dept. of Astronomy, Private Bag X3, Rondebosch 7701, South Africa
[5]Institute of Astronomy, University of Cambridge, Madingley Road, Cambridge CB3 0HA, UK

Abstract. We present several results from our analysis of dwarf irregular galaxies culled from The HI Nearby Galaxy Survey (THINGS). We analyse the rotation curves of two galaxies based on "bulk" velocity fields, i.e. velocity maps from which random non–circular motions are removed. We confirm that their dark matter distribution is best fit by an isothermal halo model. We show that the star formation properties of dIrr galaxies resemble those of the outer parts of larger, spiral systems. Lastly, we study the large scale (3–D) distribution of the gas, and argue that the gas disk in dIrrs is thick, both in a relative, as well as in an absolute sense as compared to spirals. Massive star formation through subsequent supernova explosions is able to redistribute the bulk of the ISM, creating large cavities. These cavities are often larger, and longer–lived than in spiral galaxies.

Keywords. galaxies: structure, galaxies: spiral, galaxies: ISM

1. Introduction

Dwarf irregular (dIrr) galaxies are known to be gas rich. Whereas their larger spiral cousins have gas fractions of order 10%, dIrr galaxies routinely have 50% of their baryonic mass in the gas phase. Although many dIrr galaxies are actively forming stars, and therefore must harbour at least some gas in molecular form, this phase of the ISM is elusive. Cold H_2, which makes up the bulk of GMCs, is hard to detect directly so CO emission is used as a proxy. However, the heavy element abundance of dwarfs is low which implies that the tracer molecule is scarce. Also, as a result of the low metallicity, their dust content is low which means that ionising radiation can penetrate deeper into dense clouds, at least until densities are high enough for self–shielding to become important. The upshot of all this is that no CO detection has been reported from any dwarf with a metallicity of $12 + \log[O/H] \lesssim 7.9$ (Taylor *et al.* 1998; Bolatto *et al.* 2008). Therefore, most of what we know about the gas phase in a low metallicity ISM comes from observations of the neutral, atomic phase, i.e., from H I studies, H II and dust being only minor constituents.

H I in dIrr galaxies generally extends well beyond R_{25}, the radius at an isophotal level of 25th mag arcsec^{-2}. The most extreme cases known are DDO 154 (Hoffman *et al.* 2001) and NGC 3741 (Begum *et al.* 2005). Their rotation is dominated by solid body rotation, most rotation curves barely starting to flatten by the time the last measured point is reached (de Blok *et al.* 2008). Even in their very centres, and contrary to what is found in spiral galaxies, they are dark-matter (DM) dominated (Carignan & Freeman 1988; de Blok *et al.* 2008). As their luminosity decreases, the gas fraction becomes proportionally more important to the point that at faint absolute luminosities the gas mass dominates

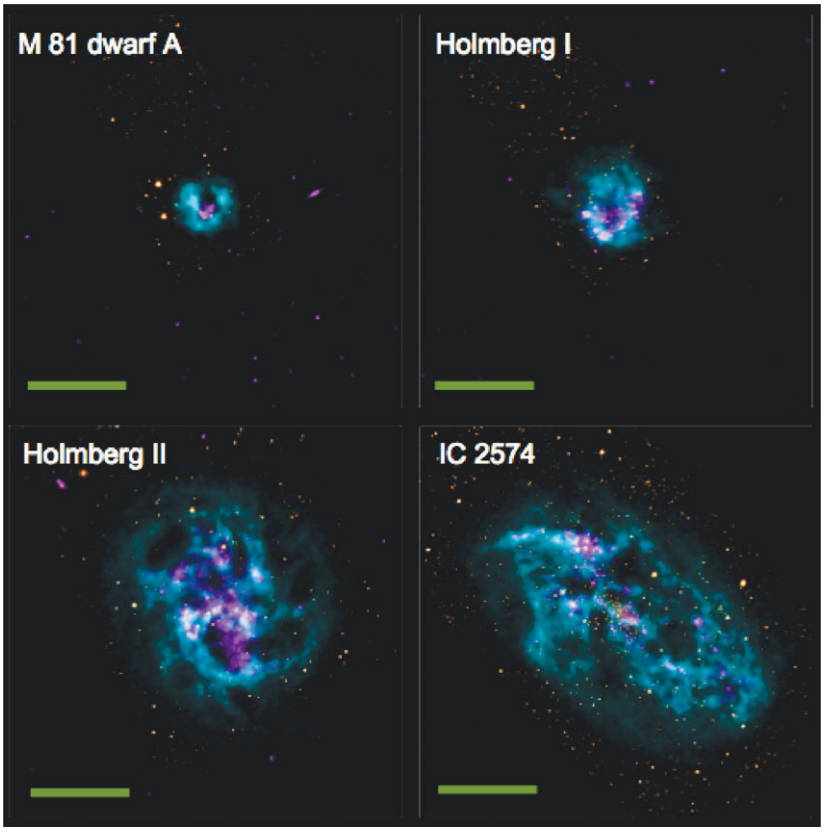

Figure 1. Some examples of dIrr galaxies, all members of the M 81 group, observed as part of THINGS. The H I emission is colour–coded in blue, the older stellar population is assigned an orange hue. Purple is a measure of the recent star formation activity and is a linear combination of the FUV flux measured with *GALEX*, and *Spitzer* 24 μm emission. The green bar measures 10 kpc. The intrinsic resolution of $\sim 6''$ at the distance of the galaxies depicted here corresponds to ~ 100 pc.

the baryonic matter budget. There seems to be a lower mass limit for H I in dwarfs of $M_{H\,I} \sim 5 \times 10^6 - 10^7$ M$_\odot$ which sets a limit to the lowest DM haloes which are able to capture and retain baryons (Taylor & Webster 2005). Even the lowest mass H I clouds have an optical counterpart; dark galaxies, i.e., DM haloes with gas but no stars, have yet to be found.

The observed velocity dispersions of H I in dwarfs is on average 6–9 km s^{-1}, but several studies have reported two components, a broad ubiquitous component of 9 km s^{-1} and a more narrow component, thought to trace cool, dense gas showing a velocity dispersion of $\sim$ 4 km s^{-1} (Young & Lo 1996, 1997; Young *et al.* 2003; de Blok & Walter 2006). Lastly, 50% of field dwarf galaxies, i.e. those not obviously being a satellite of a larger system, either have an equal mass or lower mass dwarf companion (Taylor 1997).

Several groups have embarked on surveys of large numbers of dwarf galaxies to extend the results listed above and put them on a statistically more secure footing. Recent studies based on GMRT observations have been reported by Begum *et al.* (2006) and Begum *et al.* (2008). Two new Legacy Surveys have been awarded time at the NRAO†

† The National Radio Astronomy Observatory is a facility of the National Science Foundation operated under cooperative agreement by Associated Universities, Inc.

Very Large Array (VLA), i.e. ANGST by Ott *et al.*, and LITTLE THINGS by Hunter and collaborators.

The sample described in this contribution was observed as part of THINGS, The H I Nearby Galaxy Survey (Walter *et al.* 2008), and consists of 11 LSB and dIrr galaxies. The survey was carried out with the VLA in its B–, C–, and D–configuration, resulting in maps at a spatial resolution of $6''$. The velocity resolution is $5.2\,\mathrm{km\,s^{-1}}$ or better and the observations reach typical 1σ column density sensitivities of $4 \times 10^{19}\,\mathrm{cm^{-2}}$ at $30''$ resolution. Full details regarding the observations and data reduction can be found in Walter *et al.* (2008). Most of the galaxies in THINGS were drawn from the *Spitzer*

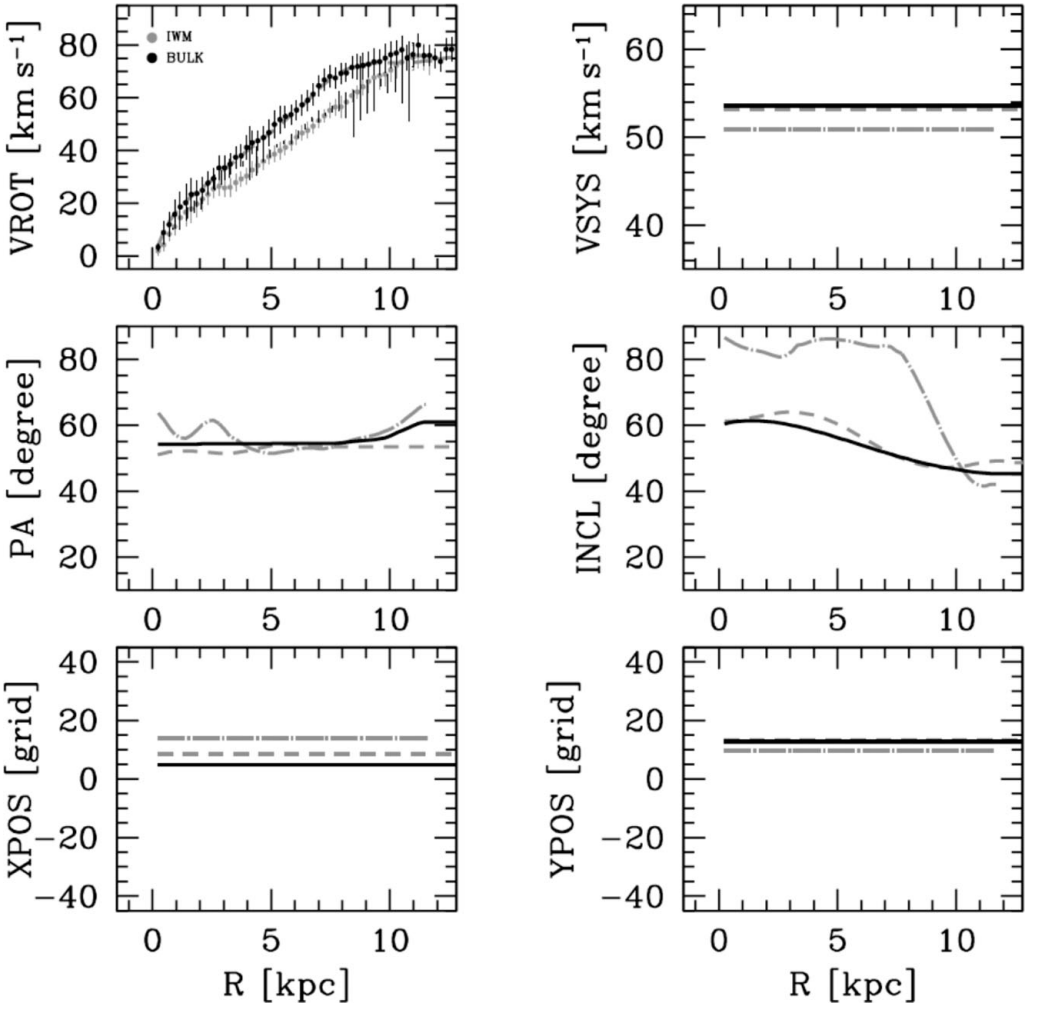

Figure 2. Tilted–ring analysis of the galaxy IC 2574 based on the bulk velocity field (top left panel; filled circles). The gray dashed lines in the other five panels are used as initial values for a tilted–ring fit to the bulk velocity field. The solid black lines show the adopted rotation curves of IC 2574 using the bulk velocity field. The fit to the bulk velocity field is compared with that based on the IWM velocity field (top left panel; filled grey circles). The gray long dash–dotted lines represent the fits of the geometrical parameters to the IWM velocity field. The large difference in inclination between IWM and bulk velocity fields is clearly evident in the panel labeled INCL and this results in a significant difference ($> 14\,\mathrm{km\,s^{-1}}$) in rotational velocity (figure taken from Oh *et al.* 2008).

Infrared Nearby Galaxies Survey (SINGS; Kennicutt *et al.* 2003), a multi-wavelength project designed to study the properties of the dusty ISM in nearby galaxies and most are also part of the *GALEX* (Galaxy Evolution Explorer) Nearby Galaxy Survey (Gil de Paz *et al.* 2007).

Fig. 1 shows a mosaic of false colour composites for four dIrr galaxies (see figure caption for details). In the sections which follow, we will highlight some of the papers which are being produced by us, notably the mass distribution and DM content of dIrr galaxies, their star formation (SF) characteristics, and the structure and morphology of their ISM.

2. Kinematics and Mass models

In the paper by de Blok *et al.* (2008) we present a rotation curve analyis of 19 THINGS galaxies. These are the highest quality H I rotation curves available to date for a large sample of nearby galaxies, spanning a wide range of H I masses and luminosities. Having said that, in the case of dwarf galaxies, motion due to gas streaming along a bar or oval distortion, or expanding shells around the site of OB associations, can give rise to quasi–random non–circular velocity components which correspond to an appreciable fraction of the rotational velocity. Ordinarily, the intensity–weighted mean velocities (IWM), or velocity fields, are affected by all these components. If one wishes to study the underlying mass distribution, one has to remove these non–circular components from the velocity field. Oh *et al.* (2008) devised a novel method to do just that and retrieve the underlying "bulk" velocity field (see their paper for details). Fig. 2 illustrates the resulting rotation curve based on the bulk velocity field and compares it with the one derived "classically", i.e., based on the IWM velocity field. The largest difference in the fitted parameters is in the inclination, which in turn translates to a considerable difference in the rotation curve and hence the inferred mass distribution.

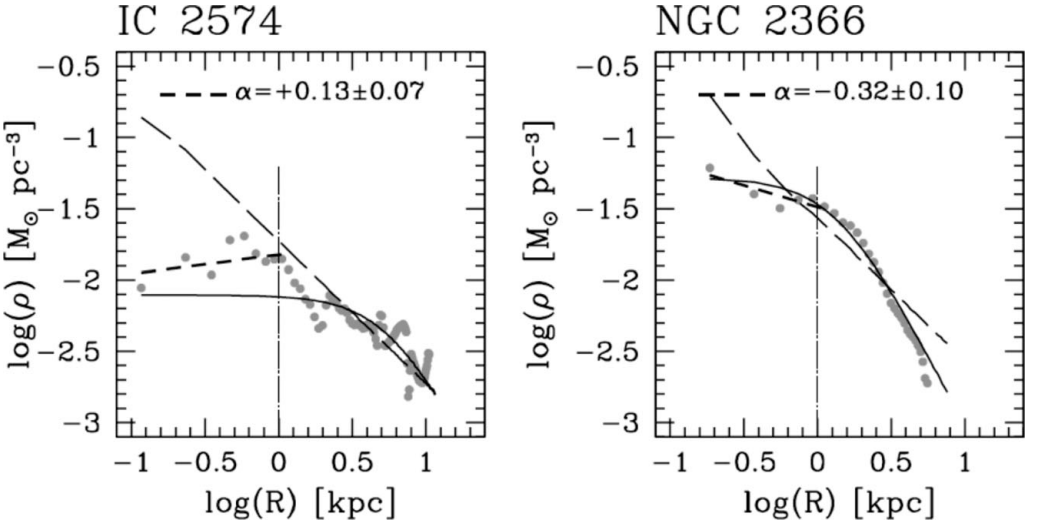

Figure 3. The derived mass density profiles of IC 2574 and NGC 2366. Long dashed and solid lines show the NFW halo model and the pseudo–isothermal halo model, respectively. Vertical long dash–dotted lines correspond to a radius of 1 kpc. The filled gray circles represent the dark matter density profile derived from the bulk rotation velocity. The inner slope of the derived dark matter density profile is denoted by α and is the result of a least squares fit (short dashed lines) to data points at radii less than 1 kpc. The measured inner slopes of the mass density profiles of IC 2574 and NGC 2366 are shown in the panels (figure taken from Oh *et al.* 2008).

Now that we have a more reliable rotation curve, less affected, if at all, by random non–circular motions, we follow the method described in de Blok & Bosma (2002) to determine the slope of the inner component of the mass density profile, $\rho \sim R^{\alpha}$. We measure the slopes, α, in plots of $\log(\rho)$ versus $\log(R)$ of the inner parts ($R < 1.2\,\mathrm{kpc}$) of IC 2574 and NGC 2366 using a least squares fit and find the values of the slopes to be $\alpha = +0.13 \pm 0.07$ for IC 2574 and $\alpha = -0.32 \pm 0.10$ for NGC 2366, respectively. This is shown in Fig. 3 and is in good agreement with the earlier result of $\alpha = -0.2 \pm 0.2$ by de Blok & Bosma (2002) for a larger sample of LSB galaxies. These flat slopes imply that the dark matter distributions of IC 2574 and NGC 2366 are well characterized by a

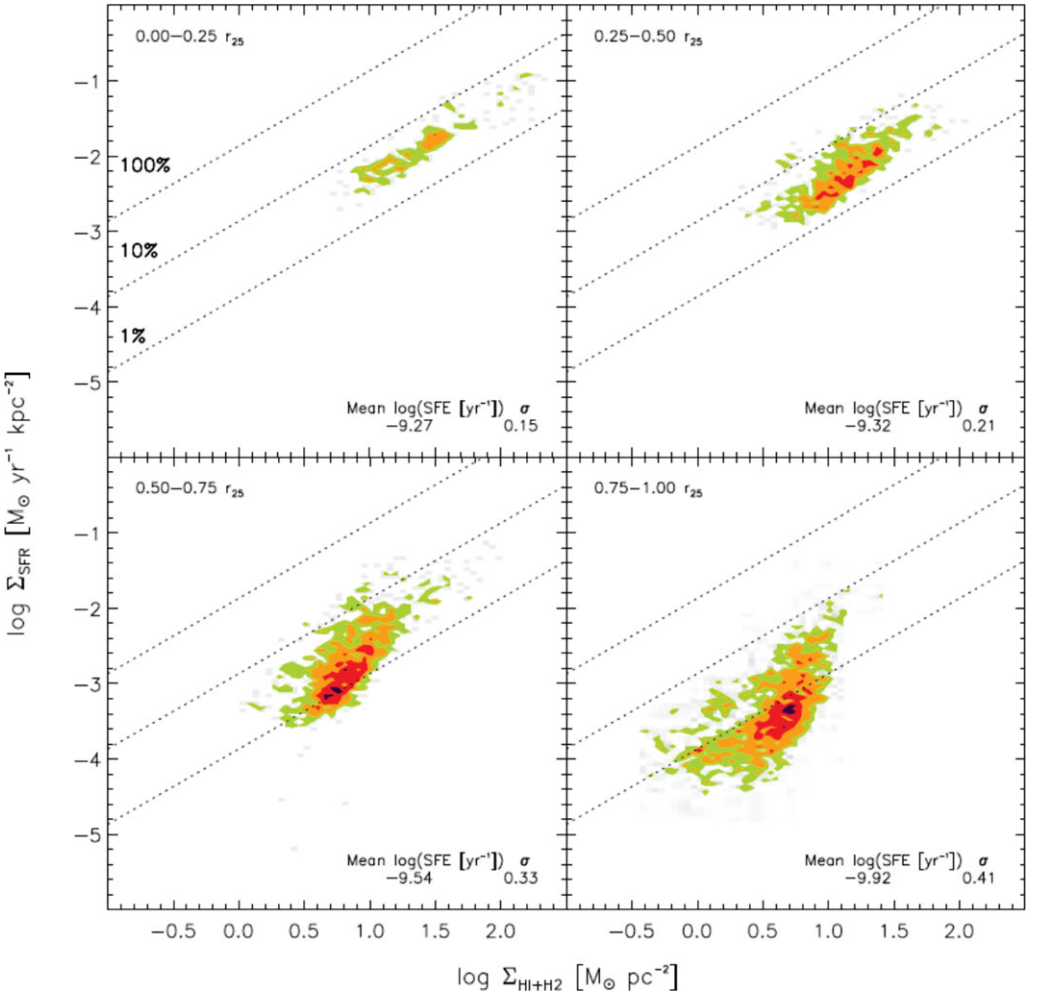

Figure 4. Variations of $\log \Sigma_{\mathrm{SFR}}$ versus $\log \Sigma_{\mathrm{H\,I+H_2}}$ with radius in spiral galaxies. The results for 7 spiral galaxies are plotted together in these diagrams. Green, orange, red, and magenta cells show contours of 1, 2, 5, and 10 independent data points per 0.05 dex–wide cell. Diagonal dotted lines show lines of constant SFE, indicating the level of SFR needed to consume 1%, 10% and 100% of the gas reservoir (including helium) in 10^8 years. Thus, the lines also correspond to constant gas depletion times of, from top to bottom, $10^8, 10^9$, and 10^{10} yr. The data are plotted in 4 radius bins: $0.0 - 0.25\,R_{25}$, $0.25 - 0.5\mathrm{R}_{25}$, $0.5 - 0.75\,R_{25}$, and $0.75 - 1.0\,R_{25}$ (figure taken from Bigiel *et al.* 2008).

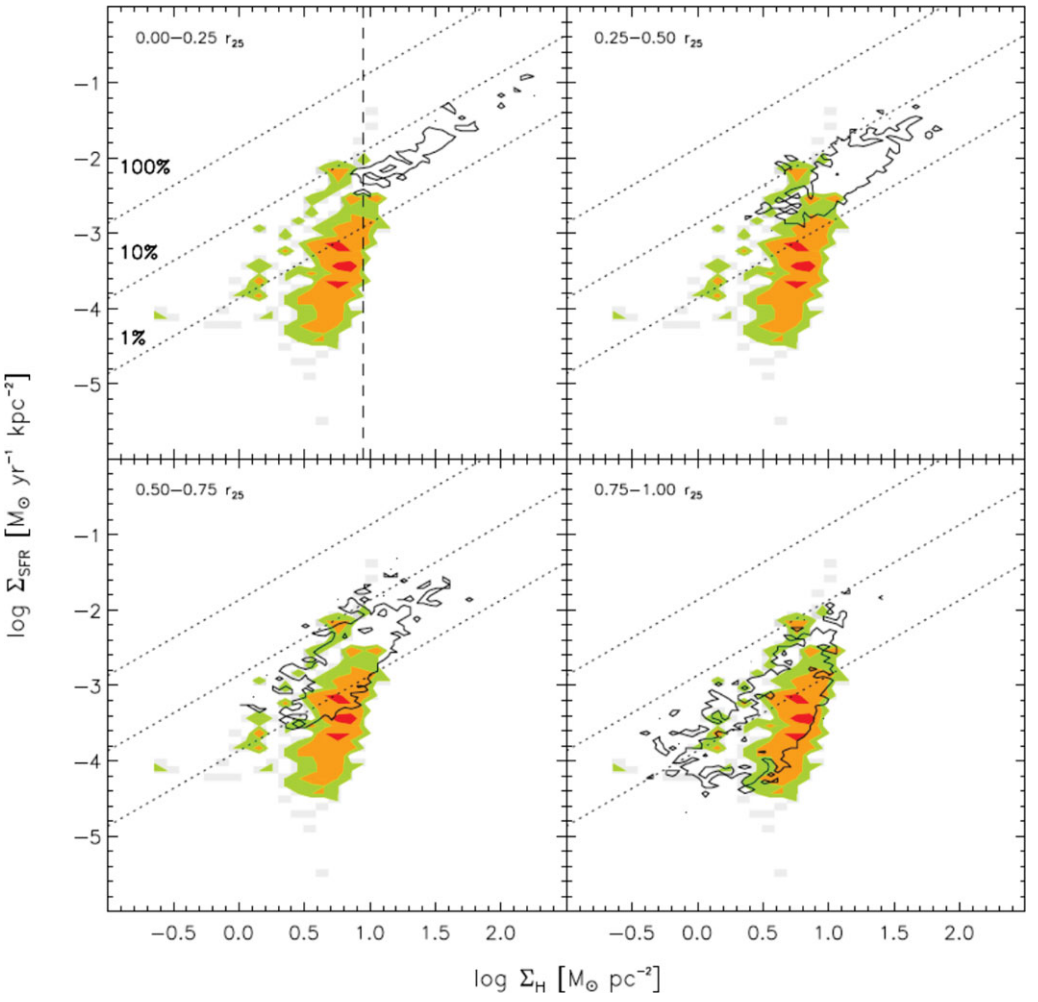

Figure 5. As Fig. 4 but for the dwarf galaxies in our sample. All four panels show the same distribution for the dIrrs. Note that the SFR density is plotted against $\Sigma_{\rm H\,I}$ (see text). Plotted over the dwarf distribution is the lowest contour for the spirals from the corresponding panel in Fig. 4. Thus each panel compares the distribution for the dwarfs to that in spiral galaxies from a particular radial range. The best agreement is seen in the bottom right panel, in which the black contour shows data from $0.75 - 1.0 R_{25}$ in spiral galaxies. The vertical dashed line in the top left panel drawn at $9\,{\rm M}_\odot\,{\rm pc}^{-2}$ locates the total gas density above which the ISM is predominantly molecular in spiral galaxies (figure taken from Bigiel *et al.* 2008).

sizeable constant-density core, for which we expect $\alpha = 0$. This is in sharp contrast with the steep slope of $\alpha = -1$ predicted by the NFW profile (Navarro, Frenk & White 1996).

3. Star Formation Law

Following Kennicutt (1989, 1998) we investigate the relation between the gas and star-formation rate (SFR) surface density. This is usually expressed in terms of a power law relation $\Sigma_{SFR} \sim (\Sigma_{gas})^N$. The value of N has been found to cover a wide range in value, from 0.9–3.5 (see Bigiel *et al.* 2008, for a summary). Kennicutt (1998) finds a value of $N = 1.40 \pm 0.15$ when plotting the disk–averaged SFR against the total

gas density (H I+H_2) in a sample of 61 nearby normal spiral and 36 infrared–selected starburst galaxies. Using THINGS we are now able to investigate the relation between SFR density and gas density on a pixel by pixel basis, the pixels being chosen to be at a common linear resolution of 750 pc, and to extend this relation to dwarf galaxies, thus probing the low–mass, low–metallicity regime. We use a linear combination of *GALEX* FUV and *Spitzer* 24 μm emission to determine the SFR (details and justification are discussed in Leroy *et al.* 2008).

We plot in Fig. 4 $\log \Sigma_{\rm SFR}$ (the log of the SFR density) against $\log \Sigma_{\rm H\,I+H_2}$ (see figure caption for details) and we do this for 4 annuli: $0.0-0.25\,R_{25}$, $0.25-0.5{\rm R}_{25}$, $0.5-0.75\,R_{25}$, and $0.75-1.0\,R_{25}$. We show in Bigiel *et al.* (2008) that when plotting $\log \Sigma_{\rm SFR}$ versus $\log \Sigma_{\rm H_2}$ we find a power law relation with $N = 1.0 \pm 0.2$ across our sample of spiral galaxies. We interpret this as indication that H_2 forms stars at a constant efficiency in spirals. The average molecular gas depletion time is $\sim 2 \times 10^9$ years. We interpret the linear relation and constant depletion time over this range as evidence that stars are forming in GMCs with approximately uniform properties and that $\Sigma_{\rm H_2}$ may be more a measure of the filling fraction of giant molecular clouds than changing conditions in the molecular gas. And because the ISM in the central regions of galaxies tends to be largely molecular, the data in the two top panels of Fig. 4, corresponding to the central and hence molecule dominated ISM, reflect this result. The bottom panels, in contrast, show the relation in the outer parts of galaxies where atomic gas prevails. This is where we see that the power law relation breaks down.

In Fig. 5 we present a very similar graph for the dwarf galaxies in our sample. Because, as mentioned earlier, H_2 is difficult to detect and assuming that, if anything, the ISM in dIrr galaxies is predominantly atomic, we used $\log \Sigma_{\rm H\,I}$ as a proxy for the total gas content of dwarfs. In each of the four panels we show the same (i.e., all) independent data points for the dwarfs as coloured contours. What changes in this figure is the contour which corresponds to the lowest contour for the spirals from the corresponding panel in Fig. 4. What we learn from this is that the star formation properties of low–metallicity, dIrr galaxies resemble those encountered in the outskirts of spiral galaxies. In the outer regions of spirals, and therefore similarly in dwarfs, HI dominates and the SF is less efficient, the efficiency decreasing monotonically with radius.

4. H I Supershells

The superior resolution and sensitivity of THINGS reveals a wealth of structure in the ISM of gas–rich systems as can be appreciated from Fig. 1. For example, Holmberg II and IC 2574 are riddled with holes in their H I distribution. These features are common in disk galaxies, including dwarfs. Studies of the LMC (Kim *et al.* 1999) by several groups quite convincingly show that many of the H I holes are cavities in the ISM filled with hot, X–ray emitting gas (Dunne *et al.* 2001, and references therein). The origin of this gas is thought to be a result of Type II supernovae from massive stars which formed in super star clusters (SSCs) or OB associations (Oey & Clarke 1997).

Bagetakos *et al.* (2008) have detected more than 1000 holes in a total of 20 galaxies selected from THINGS, in both spirals as well as in dwarfs. This is the first time that the same detection technique is applied using such a large data set of uniformly high quality. The sizes of the H I holes range from about 100 pc (our resolution limit) to 2000 pc. Their expansion velocities vary from 5 to 35 km s^{-1}. We estimate their ages at 6 – 150 Myr and their energy requirements, based on a simple single blast approximation (Chevalier 1974), at $10^{50}-10^{53}$ erg. The kinetic energy deposited is compatible with it being independent of galaxy type: an OB association is to first order oblivious to the nature of its host galaxy.

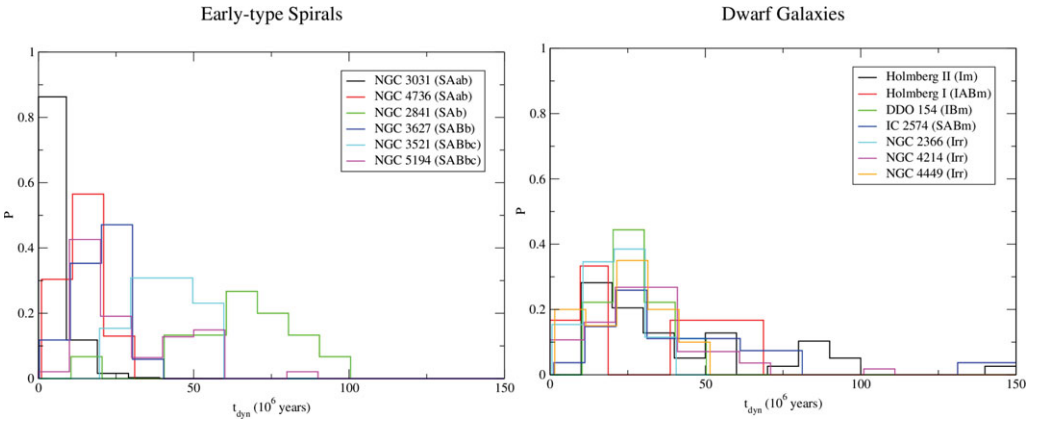

Figure 6. The number distributions of the kinematic ages of the H I holes divided into 2 different groups of galaxies: early–type spirals are pictured in the left panel and dwarf galaxies on the right. The y–axis shows the relative number distribution, P, the x–axis corresponds to the kinematic age.

In most galaxies, H I holes are found all the way out to the edge of the H I disk. Assuming that holes are the result of massive star formation we estimate the star formation rate and find that it correlates with values obtained by other SF tracers, corroborating the assertion that they are the result of the evolution of massive stars.

We find that the kinematic ages of the holes show a trend in the sense that holes in early–type spirals are younger than in dwarfs. This is illustrated in Fig. 6. This is probably due to a combination of factors: holes in spirals tend to be distorted and destroyed by the passage of spiral density waves and through shear which sets an upper limit to their age. No such mechanisms occur in dwarfs, which rotate more or less as solid bodies and lack spiral arms. Hence holes in dwarfs tend to survive for longer. We confirm that H I holes in dwarfs tend to be larger than in spiral galaxies (Brinks *et al.* 2002; Walter & Brinks 1999; Puche *et al.* 1992). This we ascribe to the fact that the mass volume density in the plane of a dIrr is lower than that of a larger spiral. Therefore, for similar observed H I velocity dispersions, the gas disk in a dwarf will be thicker, both in a relative as well as absolute sense. Because we also find that the amount of energy input is similar in dIrrs and in spirals, H I holes can grow to much larger diameters in dwarfs whereas they would suffer blow–out in the disks of spirals.

It has been argued that it would be easier for dwarf galaxies to lose a large fraction of their ISM as a result of feedback from massive star formation (Ferrara & Tolstoy 2000; Silich & Tenorio–Tagle 2001). Ott *et al.* (2005) investigated this in a sample of actively star forming dwarf galaxies. They reached the conclusion that SF activity as witnessed today in dIrrs is indeed capable of blowing enriched gas into their haloes which is then in principle able to escape. However, any extended low density envelope of material may delay this outflow on time–scales exceeding those of the cooling time of the hot gas.

References

Bagetakos, I., Brinks, E., Walter, F., de Blok, W. J. G., Rich, J. W., Usero, A., & Kennicutt, R.C., Jr. 2008, *AJ* (submitted)

Begum, A., Chengalur, J. N., & Karachentsev, I. D. 2005, *A&A*, 433, L1

Begum, A., Chengalur, J. N., Karachentsev, I. D., Kaisin, S. S., & Sharina, M. E. 2006, *MNRAS*, 365, 1220

Begum, A., Chengalur, J. N., Karachentsev, I. D., Sharina, M. E., & Kaisin, S. S. 2008, *MNRAS*, 386, 1667
Bigiel, F., Leroy, A., Walter, F., Brinks, E., de Blok, W. J.G., Madore, B., & Thornley, M.D. 2008, *AJ* (submitted)
Bolatto, A. D., Leroy, A. K., Rosolowsky, E., Walter, F., & Blitz, L. 2008, astro–ph/0807.0009
Brinks, E., Walter, F., & Ott, J. 2002, *ASP Conf. Proc.*, 275, 57
Carignan, C. & Freeman, K. C. 1988 *ApJ Lett.*, 332, L33
Chevalier, R. A. 1974, *ApJ*, 188, 501
de Blok, W. J. G. & Bosma, A. 2002, *A&A*, 385, 816
de Blok, W. J. G. & Walter, F. 2006, *AJ*, 131, 363
de Blok, W. J. G., Walter, F., Brinks, E., Trachternach, C., Oh, S.–H., & Kennicutt, R.C., Jr. 2008, *AJ* (accepted)
Dunne, B. C., Points, S. D., & Chu, Y.–H. 2001, *ApJS*, 136, 119
Ferrara, A. & Tolstoy, E. 2000, *MNRAS*, 313, 291
Gil de Paz, A., *et al.* 2007, *ApJS*, 173, 185
Hoffman, G. L., Salpeter, E. E., & Carle, N. J. 2001, *AJ*, 122, 2428
Kennicutt, R. C. 1989, *ApJ*, 344, 685
Kennicutt, R. C. 1998, *ApJ*, 498, 541
Kennicutt, R. C., Jr., *et al.* 2003, *PASP*, 115, 928
Kim, S, Dopita, M. A., Staveley–Smith, L.,& Bessell, M. S. 1999 *AJ*, 118, 2797
Leroy, A., Walter, F., Brinks, E., Bigiel, F., de Blok, W. J. G., Madore, B., & Thornley, M.D. 2008 *AJ* (accepted)
Navarro, J. F., Frenk, C. S., & White, S. D. M. 1996, *ApJ*, 462, 563
Oh, S.–H., de Blok, W. J. G., Walter, F., Brinks, E., & Kennicutt, R. C., Jr. 2008, *AJ* (accepted)
Ott, J., Walter, F., & Brinks, E. 2005, *MNRAS*, 358, 1453
Oey, M. S. & Clarke, C. J. 1997, *MNRAS*, 289, 570
Puche, D., Westpfahl, D., Brinks, E., & Roy, J.–R. 1992, *AJ*, 103, 1841
Silich, S. A. & Tenorio–Tagle, G. 2001, *ApJ*, 552, 91
Taylor, C. L. 1997, *ApJ*, 480, 524
Taylor, C. L., Kobulnicky, H. A., & Skillman, E. D. 1998 *AJ*, 116, 2746
Taylor, E. N. & Webster, R. L. 2005 *ApJ*, 634, 1067
Walter, F. & Brinks, E. 1999, *AJ*, 118, 273
Walter, F., Brinks, E., de Blok, W. J. G., Bigiel, F., Kennicutt, R. C., Jr., Thornley, M. D., & Leroy, A. 2008, *AJ* (accepted)
Young, L. M. & Lo, K. Y. 1996, *ApJ*, 462, 203
Young, L. M. & Lo, K. Y. 1997, *ApJ*, 490, 710
Young, L. M., van Zee, L., Lo, K. Y., Dohm–Palmer, R. C., & Beierle, M. E. 2003, *ApJ*, 592, 111